

A Cylindrical Micro Ultrasonic Motor Using PZT Thin Film Deposited by Single Process Hydrothermal Method (ϕ 2.4 mm, L = 10 mm Stator Transducer)

Takeshi Morita, Minoru Kuribayashi Kurosawa, *Member, IEEE*, and Toshiro Higuchi, *Member, IEEE*

Abstract—A micro ultrasonic motor using PZT (lead zirconate titanate) thin film has been improved by a single process hydrothermal method. The hydrothermal method is a unique method for depositing PZT thin film in a solution. An earlier reported hydrothermal method consisted of two linked processes. Our new method, however, has only a single process. Hence, less distribution of chemical components of the PZT film contributes to a higher efficiency of the stator transducer. The piezoelectric factor d_{31} was -30 pC/N for this new method, which is six times larger than that of the previous method. The output torque of the micro ultrasonic motor fabricated by the single process hydrothermal method was measured. The output torque was 7.0 μ Nm, and the maximum revolution speed was 880 rpm at 15 Vp-p driving voltage.

I. INTRODUCTION

ULTRASONIC MOTORS are distinguished by a performance of high torque with low speed. Therefore, an ultrasonic micro motor would have advantages over other motors such as electrostatic motors [1]–[3] or magnetic motors [4] when applied to micro mechanical systems. Furthermore, ultrasonic motors have a simple structure and require no complicated gear box.

In particular, a cylindrical-type motor has larger mechanical output power than a disk-type ultrasonic motor in cm-order [5]. This also may be true in mm-order and sub mm-order. A cylindrical micro ultrasonic motor fabricated by a hydrothermal method [6], [7] was developed in 1995 [8]. However, the motor has no preload mechanism. The piezoelectric effect of the thin film was not enough.

In fabricating disk-type [9]–[11] or cylindrical-type ultrasonic micro motors, the performance of motors depends heavily on piezoelectric thin film. Development of a piezoelectric thin film contributes not only to our motor but also to other type actuators such as a disk-type ultrasonic motor or a linear-type micro motor. In this paper, the improvement of the micro ultrasonic motor will be discussed.

Manuscript received September 2, 1997; accepted March 19, 1998.

The authors are with the Department of Precision Machinery Engineering, Graduate School of Engineering, The University of Tokyo, 7-3-1 Hongo, Bunkyo-ku, Tokyo 113-8656, Japan (e-mail: morita@intellect.pe.u-tokyo.ac.jp).

II. HYDROTHERMAL METHOD

The hydrothermal method is one of the promising methods for depositing PZT thin film on a titanium substrate. This method was reported by Shimomura *et al.* [6] in 1991. The chemical reaction between a titanium substrate and ions melted in a solution is carried out at high temperature and pressure conditions. The reaction temperature is from 100 to 200°C. Hence, the container must be sealed to prevent the solution from evaporating. Compared to other methods such as sol-gel method [12], chemical vapor deposition (CVD) [13], or the sputtering method [14], [15], the hydrothermal method has many merits as follows.

- A substrate that has curved surfaces is available. Other methods are useful only for a flat-figure substrate. The hydrothermal method, however, utilizes a chemical reaction between the substrate and ions melted in the solution, so a PZT thin film is deposited over the entire surface. This feature is essential to applying the PZT film to our cylindrical micro motor and other complicated structures.
- During the deposition, the poling direction is aligned. The direction of the chemical reaction is vertical to the surface of the titanium substrate. It has been assumed that this is why poling direction is aligned. However, a detailed explanation of this phenomenon is not yet available.
- The resulting PZT film is thick. When using other methods, the deposited PZT thin film must be annealed above 500 degrees to be crystallized. Therefore, a thick PZT film causes a clack because of the difference in the thermal expansion coefficient between PZT and the substrate. The hydrothermal method utilizes a recrystallization reaction, so annealing is not necessary and a thick film can be realized. Thicker film can endure against higher input voltage without breakdown. This advantage leads to higher output force generated by an electrical field.

III. PREVIOUS HYDROTHERMAL METHOD

The previously reported hydrothermal method [6], [7] consists of two processes, namely, a nucleation process and

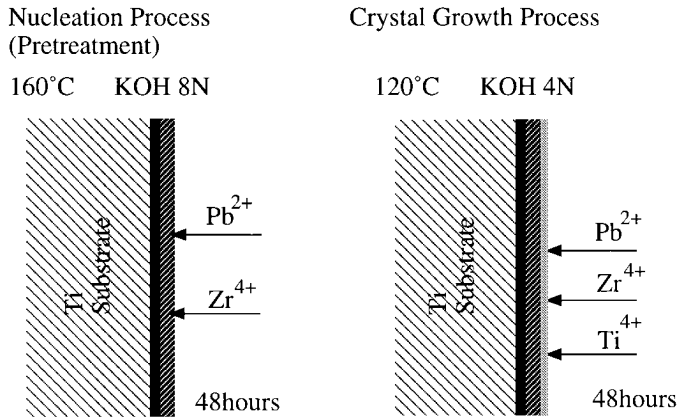


Fig. 1. Schematic explanation of the previous hydrothermal method.

TABLE I

THE REACTION CONDITIONS FOR THE EARLIER METHOD [6].

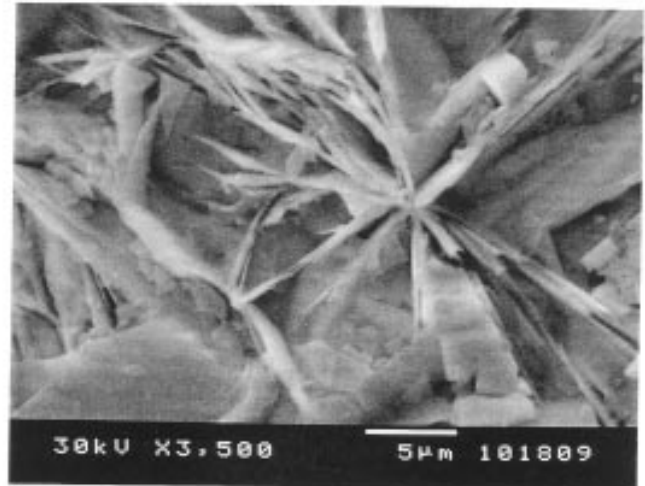
	Nucleation process	Crystal growth process
Component ions	Pb, Zr	Pb, Zr, Ti
KOH	8 N 12 ml	4 N 12 ml
Temperature	160 degrees	120 degrees
Time	48 hours	48 hours

a crystal growth process. Fig. 1 shows a schematic explanation of these processes. Shimomura *et al.* [6] and Ohba *et al.* [7] have explained the role of each process as follows. The nucleation process results in an adhesive force between the titanium substrate and the deposited thin film. The titanium ions are supplied by the substrate, and the other ions (Pb^{4+} , Zr^{4+}) are supplied by the solution. The crystal growth process makes it easy to control the chemical composition because all ions are supplied from the solution.

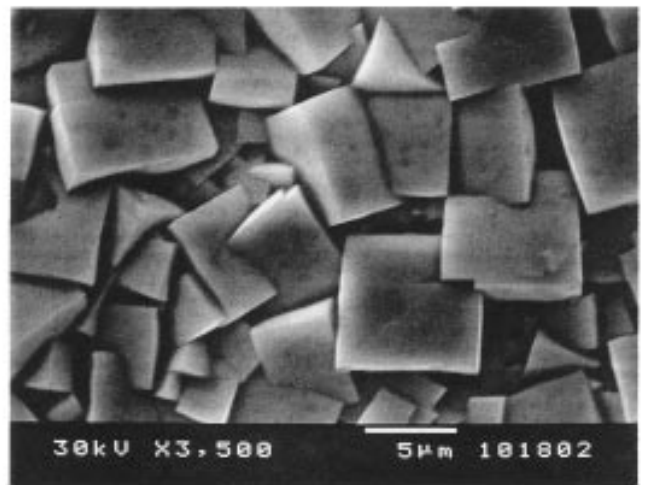
Not only the ions but also the concentrations of alkali and the reaction temperatures are different between the two processes, as shown in Table I. The reaction time for the previous method is 48 hours; and, for thick film, the crystal growth process is carried out repeatedly.

We have found that, in the nucleation process, separated PT and PZ layers are deposited. The reaction conditions were given in the previous report [6], [7]. Fig. 2 shows scanning electron microscope (SEM) photographs of the films deposited by a nucleation process for 2 hours (a) and for 48 hours (b). These photographs show obviously different crystals. An energy dispersive X-ray spectrometry (EDX) analysis indicated that the crystals deposited first were PT, and the next crystals were PZ. The X-ray diffraction pattern of the deposited thin film for 48 hours is shown in Fig. 3. The PT deposition took place for about 2 hours. It seems that, during the first 2 hours, the PT film was deposited, then PZ film was deposited on PT film. Therefore, a part of the film was almost entirely PZ.

The crystal growth process was carried out for 24 hours after the nucleation process (24 hours) as reported, as opposed to 48 hours. The results did not change because of the different reaction time. The SEM photograph is shown



(a)



(b)

Fig. 2. SEM photograph of thin film deposited for (a) 2 hours and (b) 48 hours by a nucleation process.

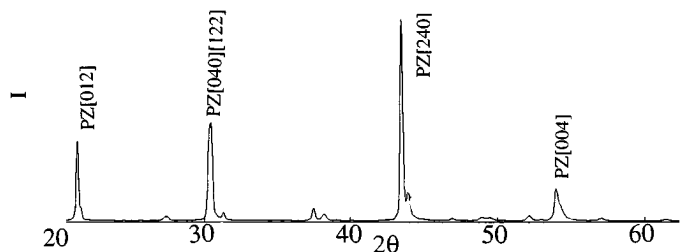


Fig. 3. XRD pattern of thin film deposited by a nucleation process.

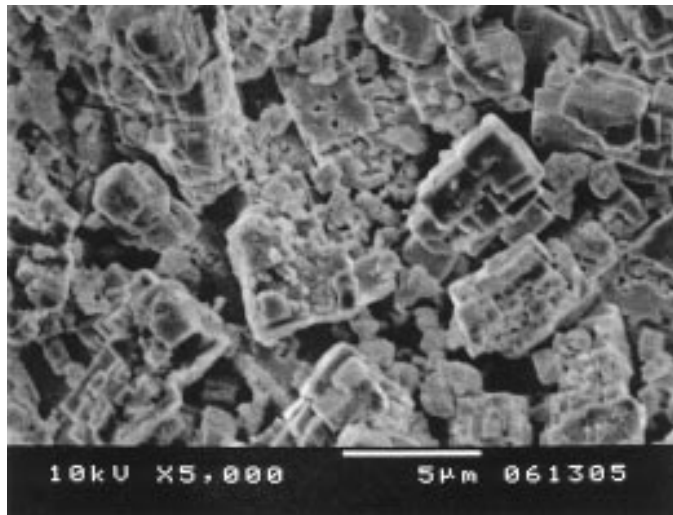


Fig. 4. SEM photograph of thin film deposited by a crystal growth process after the nucleation process.

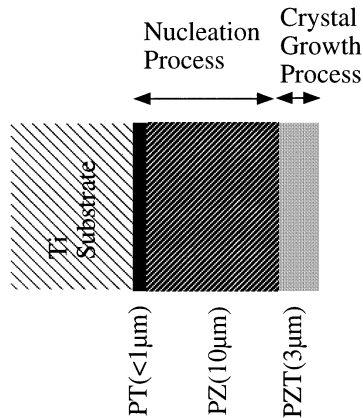


Fig. 5. Schematic explanation of the single process hydrothermal method.

in Fig. 4. The X-ray diffraction pattern (XRD) and the EDX confirmed that the chemical composition of the thin film deposited by the crystal growth process was PZT. During the crystal growth process, the reaction only occurred on the PZ film. It was impossible to deposit the PZT thin film by the crystal growth process on the titanium substrate or on the PT film deposited on titanium. Therefore, the nucleation process was essential. It seems that the composition of the thin film deposited by the earlier hydrothermal method results in a complicated distribution in the direction of deposition, as shown in Fig. 5. The thin film deposited using only the nucleation process has a minimal piezoelectric effect because it is not PZT.

IV. NEW HYDROTHERMAL METHOD

The distribution of chemical components in the direction of deposition should be uniform. To simplify the hydrothermal method, it is possible to deposit a PZT thin film by a single process. By changing the reaction temperature, the concentration of ions, and the KOH concentra-

Single process

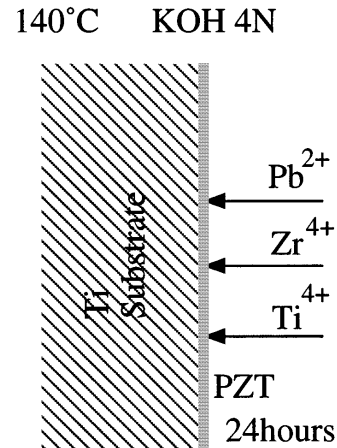


Fig. 6. Cross-section of thin film deposited by the previous hydrothermal method.

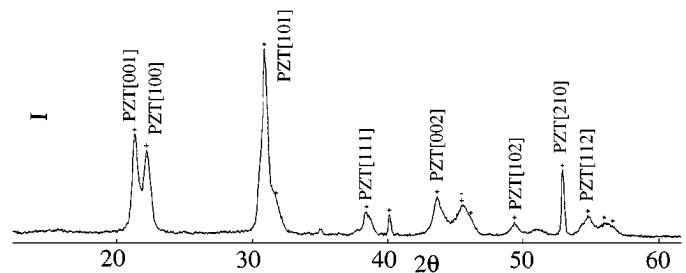


Fig. 7. XRD pattern of thin film deposited by the single process hydrothermal method.

tion, the PZT thin film is successfully deposited directly on a titanium substrate, as shown in Fig. 6. The result of the XRD analysis indicated that the film was PZT, as shown in Fig. 7. The SEM photograph of this film shows that the crystals deposited by the new process were cubic, as shown in Fig. 8. These crystals were two or three times smaller than the PZ crystals deposited by the nucleation process. A spontaneous polarization was confirmed by applying it to an ultrasonic micro motor, as described later. The adhesive force between the thin film and the substrate was sufficient, and the chemical composition was controllable.

The solution in the new process contains Pb, Zr, and Ti ions with concentrations almost half what they were for the crystal growth process of the previous method. In this paper, the basic reaction conditions for method are defined as shown in Table II. The substrate was a titanium plate with dimensions approximately $10 \times 50 \times 0.2 \text{ mm}^3$. The thickness was measured by a micrometer. The precise square of the titanium substrate was calculated from its weight, thickness, and density. The reaction was carried out in a mini autoclave to guard against high temperature and pressure. The volume capacity was 60 ml. The container was Teflon to prevent impurities from contaminating the solution. The autoclave was rotated at 8 rpm to make the contact between the solution and the titanium

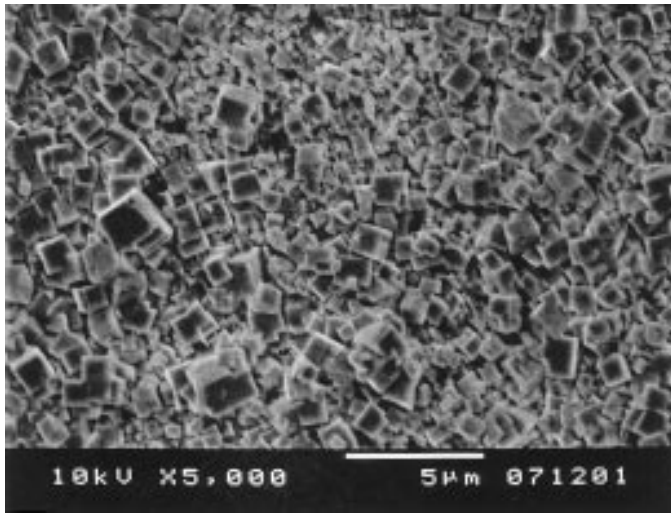


Fig. 8. SEM photograph of thin film deposited by the single process hydrothermal method.

TABLE II
THE REACTION CONDITIONS FOR THIS RESEARCH (BASIC CONDITIONS).

New Process			
Component ions	Pb ($\text{Pb}(\text{NO}_3)_2$)	0.52 mol/l	7.0 ml
	Zr ($\text{ZrOCl}_2 \cdot 8\text{H}_2\text{O}$)	0.79 mol/l	2.0 ml
	Ti (TiCl_4)	3.7 mol/l	0.39 ml
KOH		4 N	12 ml
Temperature		140 degrees	
Time		24 hours	

substrate uniform. To determine one condition (for example, the ionic concentration or the reaction time), only one parameter was varied and all others were fixed.

We found that the quantity of deposited material was affected by the concentrations of the melted ions (Pb, Zr, and Ti). The KOH concentration was fixed at 4 N. The concentrations of other ions were varied, and the ratio was kept fixed. The evaluation was based on the weight gain per unit square of the titanium plate substrate. The results are shown in Fig. 9. A cross axle was normalized to basic conditions, as shown in Table II.

A thicker solution decreased the weight of the deposited PZT. The thicker solution produced copious amount of precipitate, which prevented contact between the solution and titanium substrate. However, a thinner solution was not able to deposit a thin film and only melted the titanium substrate. To increase the film weight gain, the concentrations of the ions should be equal to those under basic conditions.

In the earlier method, the reaction time for each process was 48 hours, though the reason for this was not clear. To determine the reaction time for the new process, the relationship between the weight of the deposited film and the reaction time was studied. The result shows that the deposition was saturated after 24 hours, as shown in Fig. 10. Therefore, the reaction time was estimated to be 24 hours.

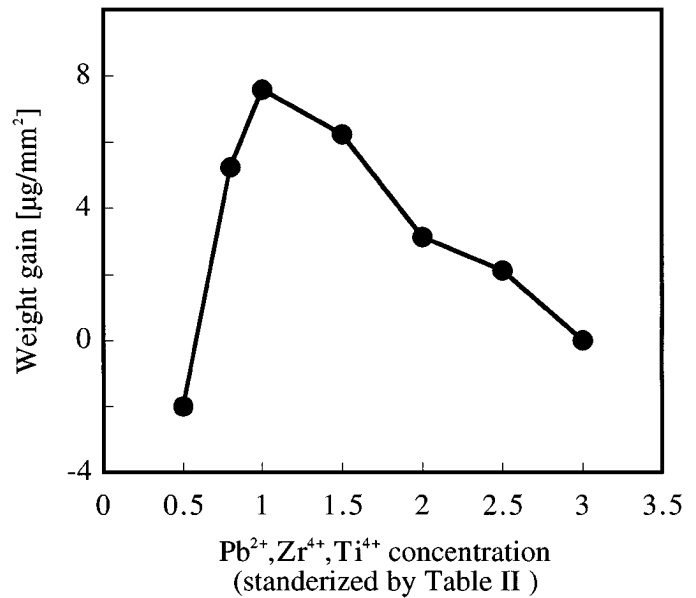


Fig. 9. The relationship between ionic concentration and weight gain for PZT thin film.

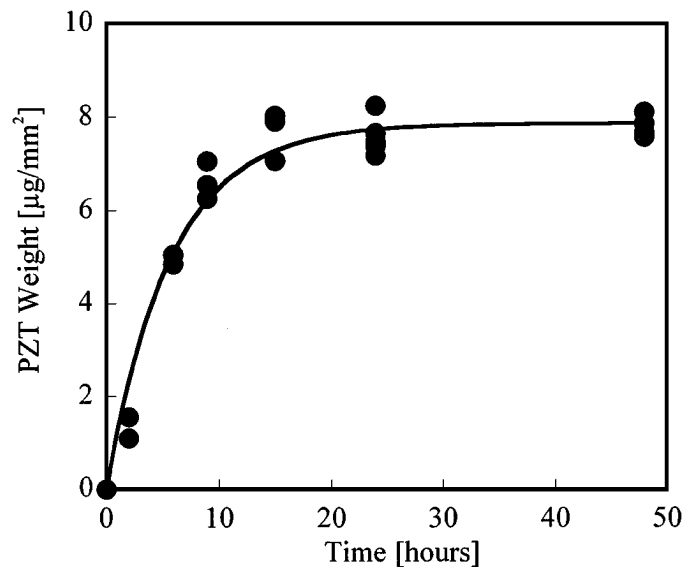


Fig. 10. The weight gain for PZT thin film versus reaction time.

The piezoelectric effect is greatly dependent on the $\text{Zr}/(\text{Ti}+\text{Zr})$ ratio of the PZT crystal. As is well-known, when the $\text{Zr}/(\text{Ti}+\text{Zr})$ ratio is 0.52, the material is called MPB (morphotropic phase boundary), and the piezoelectric constant achieves a maximum value. To control this ratio in the deposited film, the concentrations of Ti and Zr ions were changed as shown in Fig. 11. The result indicates that the $\text{Zr}/(\text{Ti}+\text{Zr})$ in a deposited crystal was roughly controllable by changing the $\text{Zr}/(\text{Ti}+\text{Zr})$ ion ratio in the solution. There was a linear relation between these two factors. As described in Section V, to increase the piezoelectric factor, only $\text{Zr}^{4+}/(\text{Zr}^{4+}+\text{Ti}^{4+})$ control is insufficient, and exact KOH concentration control also is important.

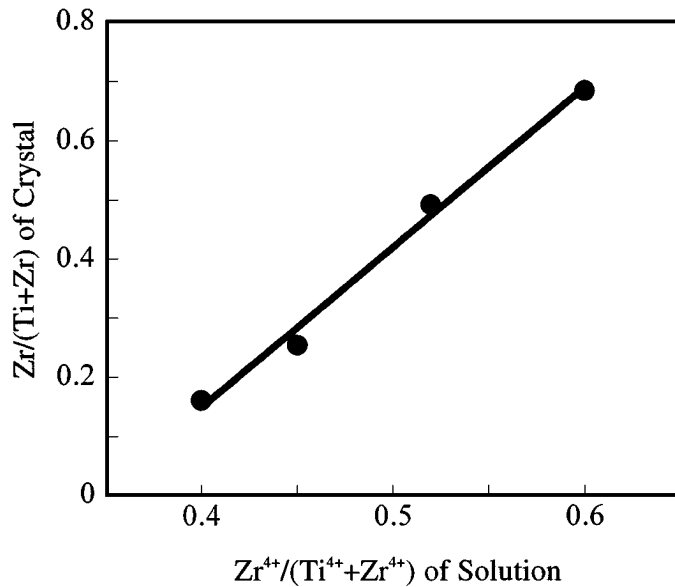


Fig. 11. A control of the chemical component of PZT thin film by a concentration ratio ($Zr^{4+}/(Zr^{4+}+Ti^{4+})$).

V. FURTHER IMPROVEMENT OF PZT

We found that the piezoelectric characteristics of the PZT film depend strongly on the concentration of KOH. PZT thin film was deposited on a titanium substrate $50\text{ mm} \times 10\text{ mm} \times 50\text{ }\mu\text{m}$ in size. The varied parameter was the weight of KOH melted into 11 ml of pure water. The ratio of $Zr^{4+}/(Zr^{4+}+Ti^{4+})$ melted into the solution was 52% and 58%. Other parameters such as reaction temperature (140 degrees) and reaction time (24 hours) were fixed as shown in Table II. The depositions were carried out twice to thicken the film. The final thickness was approximately $6\text{ }\mu\text{m}$.

The gold electrodes were fabricated on both sides by vacuum evaporation. One end of this bimorph was held, so the length was 40 mm. The driving voltage to each electrode was 200 mV_{p-p} with a 180 degree phase shift. The electrical ground was the titanium substrate. The laser spot of a laser Doppler vibrometer was irradiated to the free edge of the bimorph as shown in Fig. 12. The generated vibration mode was the first bending mode, and the amplitude, measured at the resonance frequency, was approximately 25 Hz.

As shown in Fig. 13, the precise minute change of the KOH concentration greatly affected the amplitude of the bimorph. Based on these results, the $Zr^{4+}/(Zr^{4+}+Ti^{4+})$ ratio should be 58% for a higher piezoelectric effect.

Two peaks of each graph in Fig. 13 seem to be caused by the reaction times. In this experiment, the two reactions were carried out in succession. The optimum KOH concentration of each reaction, namely the first deposition on titanium substrate and the second deposition on PZT film, seems to be different. The KOH concentration was changed between the first deposition and the second deposition, as shown in Table III. The bimorph was vibrated at 5 Hz, which is far from the resonance frequency. The input

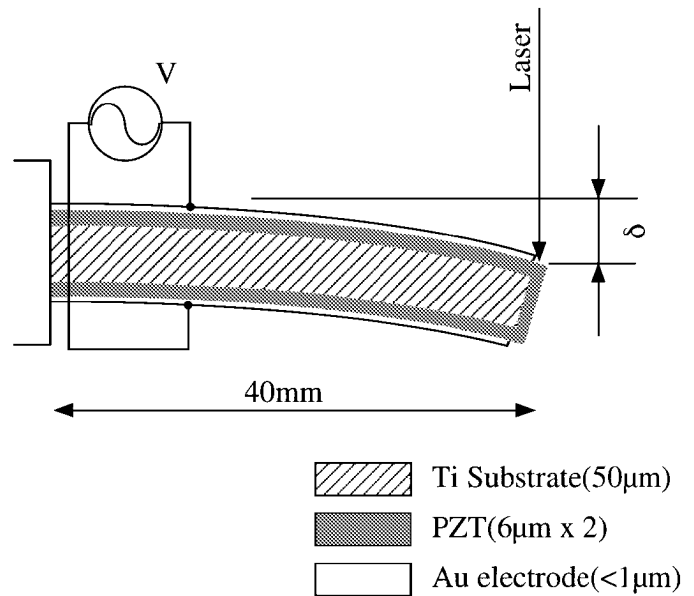


Fig. 12. Cross-section of fabricated bimorph.

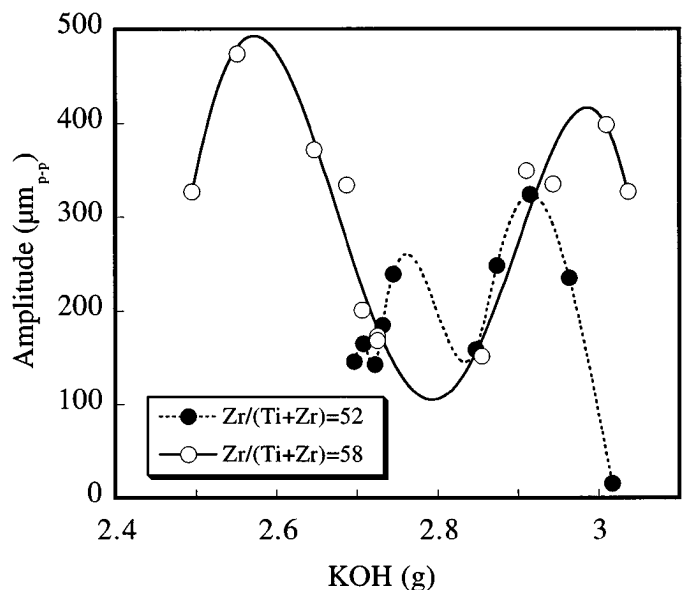


Fig. 13. The amplitude of the bimorph versus KOH concentration.

TABLE III
KOH CONCENTRATION TO FABRICATE IMPROVED BIMORPH.

	1st deposition	2nd deposition
KOH (melted into 11ml H ₂ O)	2.578 g	2.976 g
$Zr^{4+}/(Zr^{4+}+Ti^{4+})$	58%	58%

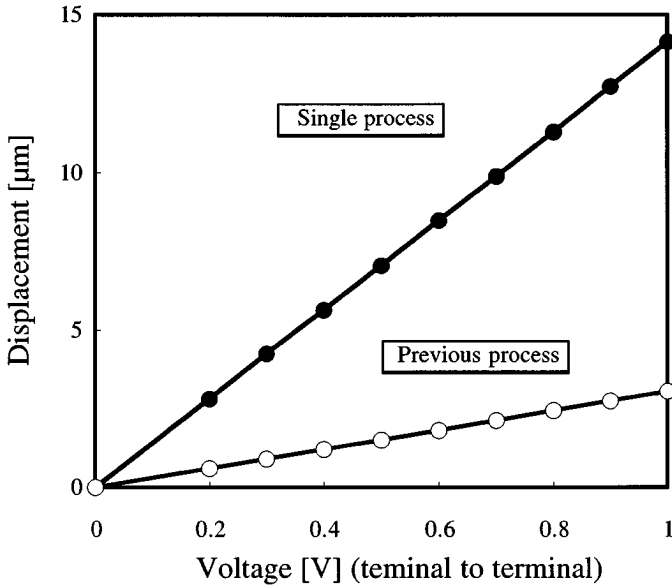


Fig. 14. A comparison of bimorph amplitude between the previous method and the single process hydrothermal method.

voltage could be regarded as DC input. The result is shown in Fig. 14 with the amplitude of the bimorph fabricated by the previous hydrothermal method. The displacement δ of the bimorph can be expressed as:

$$\delta = \frac{3l^2}{2t} \frac{(1-a^2)Y_f}{a^3Y_s + (1-a^3)Y_f} d_{31}E, \quad \left(a = \frac{t_s}{t}\right) \quad (1)$$

where l , t , t_s , Y_f , Y_s , d_{31} , and E are length, thickness of the bimorph, thickness of titanium, Young's module of PZT, Young's module of titanium, the piezoelectric factor, and electrical field, respectively [7]. The piezoelectric factor d_{31} of the PZT thin film deposited by the single process hydrothermal method is calculated to -30 pC/N, which is three times smaller than that of bulk PZT. To increase this value of PZT film, we are trying some additional experiments.

VI. STRUCTURE AND PRINCIPLE

The micro ultrasonic motor has a cylindrical stator transducer and two rotors that contain a preload mechanism. A photograph of the motor used in this study is shown in Fig. 15. The stator transducer was 2.4 mm in diameter and 10 mm long, as shown in Fig. 16. A PZT deposition was carried out two times, so the thickness of the film was about $6 \mu\text{m}$. The poling direction is the thickness direction, namely from the surface of the PZT thin film to the titanium substrate. The stator transducer is vibrated using two RF electrical sources with a 90 degree phase difference. The stator transducer is vibrated as shown in Fig. 17. The traveling wave on the top and bottom surfaces drives objects in contact with the stator by frictional force. The structure composed of the rotors and the stator are shown in Fig. 18. Mode-rotation-type cylindrical ultra-



Fig. 15. A photograph of the cylindrical micro ultrasonic motor.

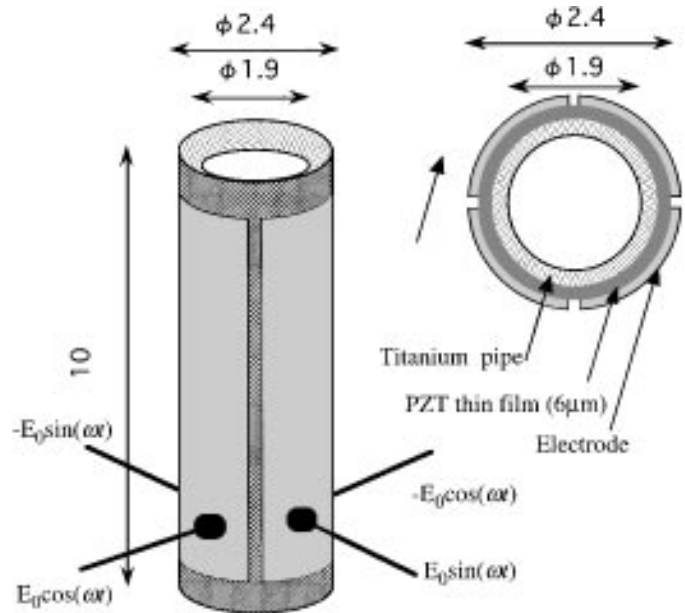


Fig. 16. Structure of the stator transducer of the micro ultrasonic motor.

sonic motors have a larger mechanical power output than a disk-type [9]–[11], although the previous motor fabricated by the previous hydrothermal method (only a nucleation process) could drive only a tiny screw placed on the stator vibrator without additional preload.

The motor shape is designed to efficiently convert vibrational energy to mechanical output [16]. It is important to make the rotor contact the stator smoothly with sufficient contact pressure. One of the authors has reported that high pressure is important to drive a slider by frictional force [17]. Therefore, the contact surfaces of the stator were fabricated like a conic, and the rotors were spherical shaped. An FEM calculation determined the ideal taper angle to be 25.5 degrees, which would prevent a slip in the radial

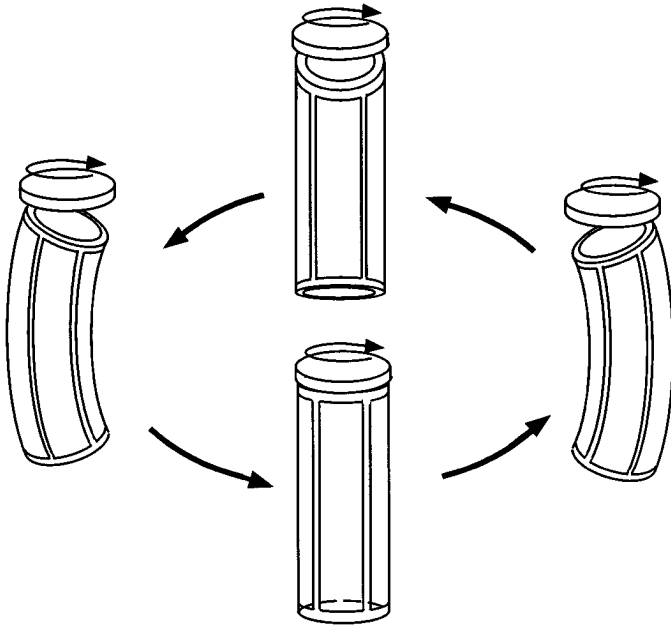


Fig. 17. A principle of the cylindrical ultrasonic motor.

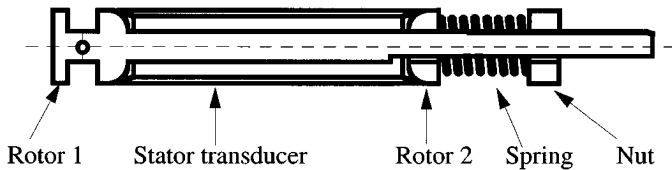


Fig. 18. Cross-section of the motor with a preload mechanism.

direction between the rotors and the stator while operating. The new motor includes a spring to press the stator from up and bottom surfaces, although previously the load pressure was only the rotor's own weight.

VII. THE PERFORMANCE OF STATOR TRANSDUCER

PZT thin film was deposited on the side wall of the stator transducer. To compare variations in the hydrothermal method, three types of stator transducers were fabricated. Other fabrication processes such as preparing titanium substrate or fabricating an electrode by evaporation were the same for each type. Each reaction conditions to deposit PZT (or PT and PZ) was as follows:

Type 1—a nucleation process	48 hours
Type 2—a nucleation process	48 hours
+ a crystal growth process	+ 48 hours
Type 3—single process (New process) 2 times	24 hours × 2

It should be noted that the total reaction times for Type 1 and Type 3 were 48 hours, and for Type 2 was 96 hours. The driving voltage was 5 V_{p-p} to one facing electrode, and the other two electrodes were open. The vibration amplitude was measured by a laser Doppler Velocimeter. The laser was irradiated to the top of the stator transducer's side wall. During this experiment, the rotors were not put on the stator transducer. The results shown in Fig. 19 indicate that the vibration amplitude of Type 3 is 2.5 times

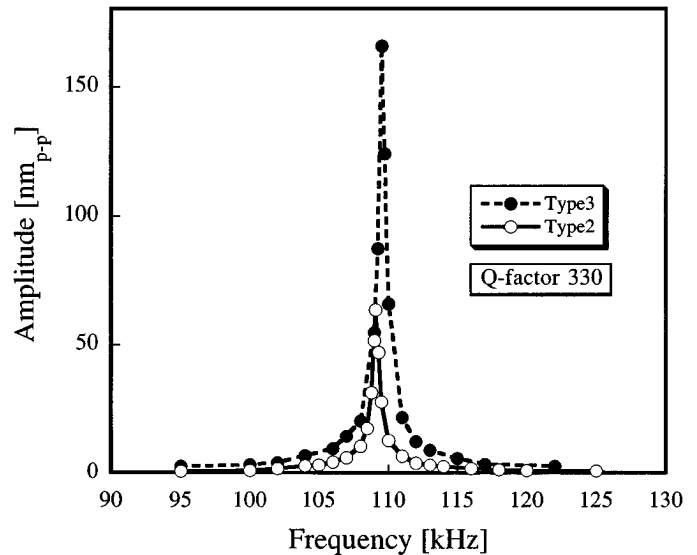


Fig. 19. The amplitude of the stator transducer versus driving frequency.

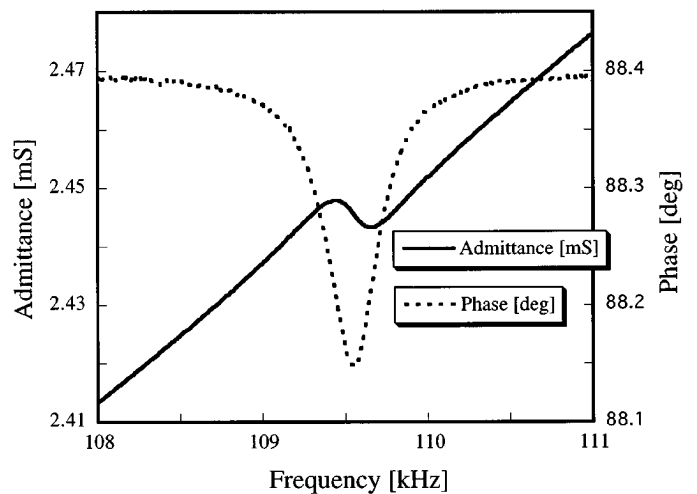


Fig. 20. The electrical characteristics of the stator transducer.

larger than that of Type 2. The Q-factor of Type 3 stator transducer was about 330. The small vibration amplitude for Type 1 indicates that the chemical component of the thin film is not PZT but PT and PZ.

VIII. EQUIVALENT CIRCUIT

The electrical characteristics of the Type 3 transducer were measured with an impedance analyzer (HP 4194A). The admittance curve and phase angle are shown in Fig. 20. The presence of a resonant peak and an antiresonant peak is confirmed. The resonance frequency 109.6 kHz was equal to the result of the measurement of the laser Doppler vibrometer. The changes in the admittance and phase angles at the resonant frequency were too minute to determine the equivalent L, C, and R elements. The changes were minute because the volume ratio of PZT thin film in relation to the entire stator transducer was small.

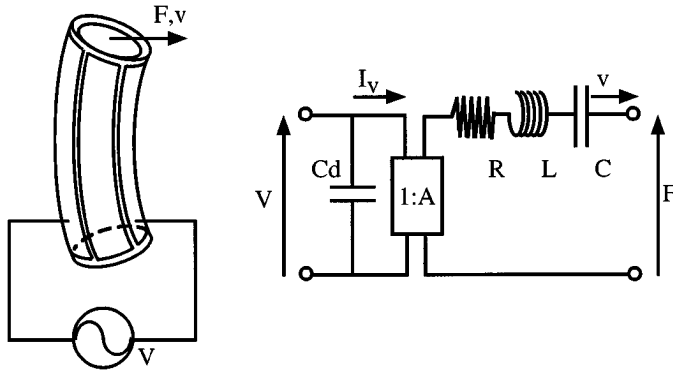


Fig. 21. The equivalent circuit for the stator transducer.

As is well-known, the resonance phenomenon can be expressed as an equivalent circuit, which is shown in Fig. 21. The force factor A relates the electrical arm to the mechanical arm at the resonance frequency as follows:

$$AV = F + Rv$$

$$I_v = Av$$

where V , I_v , F , and v are voltage, motional current, force, and the vibration velocity at the top of the stator transducer.

The equivalent elements can be obtained by calculation. The equivalent mass M ($= L$) is calculated from this equation:

$$\frac{1}{2}M \left\{ v \left(\frac{1}{2}l \right) \right\}^2 = \int_{-\frac{1}{2}l}^{\frac{1}{2}l} \frac{1}{2}v^2(z)S\rho dz$$

$$v(z) = \frac{du(z)}{dt}$$

$$u(z) = C \left(\sin \frac{\alpha}{2} \cosh \frac{\alpha}{l}z - \sinh \frac{\alpha}{2} \cos \frac{\alpha}{l}z \right) e^{j\omega t}$$

where $u(z)$ is the deformation of the amplitude of the stator transducer, namely, the vibration mode. A coordinate z is parallel to the axis of the stator transducer, and l means the length ($-\frac{1}{2}l < z < \frac{1}{2}l$).

The equivalent stiffness K ($= 1/C$) is expressed by:

$$fr = \frac{1}{2\pi} \sqrt{\frac{K}{M}}$$

where fr is the resonance frequency. The mechanical loss η ($= R$) is calculated from the Q factor obtained from the relation between the amplitude and the driving frequency near the resonance frequency:

$$R = \frac{\sqrt{KM}}{Q}$$

TABLE IV
ESTIMATED EQUIVALENT ELEMENTS.

M	15.2 mg	L	15.2 mH
K	7.22×10^6 N/m	C	$0.138 \mu\text{F}$
η	3.18×10^{-2} Ns/m	R	$3.18 \times 10^{-2} \Omega$
		C_d	3.76 nF
		ϵ	460
		$\tan \delta$	4.50%

The damped capacitance C_d was obtained from the measurement of the admittance curve, excluding the resonance frequency. With the thickness of the PZT film and the area of the electrodes, the relative dielectric coefficient was estimated to be 460. The dielectric loss tangent was 4.5%. Estimated equation elements are summarized in Table IV.

Force factor A can be obtained from the ratio between the vibration velocity and the input voltage. The boundary condition is no preload (no rotor), which means that a mechanical arm is considered too short. So:

$$F = 0$$

and

$$A = \frac{Rv}{V}$$

is calculated to be 3.6×10^{-4} N/V, which shows the maximum output force of the stator transducer. With 30 Vp-p input voltage (15 Vp-p to each electrode), the output force F and output torque are estimated to 10.8 mN and 26.0 μNm . The output torque is equal to $2Fr$, where r is the outer radius of the stator. The rotors are driven by the top and bottom faces, so the output torque is not Fr but $2Fr$.

Force factor A also can be obtained deductively using the piezoelectric equation,

$$A = \frac{I}{v} = \frac{4\sqrt{2} \left(\frac{\alpha}{l} \right) \left(r + \frac{d}{2} \right) (r + d) \sinh \frac{\alpha}{2} \sin \frac{\alpha}{2}}{\sin \frac{\alpha}{2} \cosh \frac{\alpha}{2} - \sinh \frac{\alpha}{2} \cos \frac{\alpha}{2}} d_{31} c_{11}^E$$

where α , d , and c_{11}^E are a constant (4.73), the thickness of the thin film, and Young's module of PZT thin film, respectively, supposing a piezoelectric factor d_{31} of the PZT thin film to be equal to that of the bulk (-90 pC/N), the force factor is 2.9×10^{-3} N/V, which is eight times larger than the force factor for the equivalent circuit described above. Therefore, it is clear that the PZT thin film can be improved.

When the PZT thin film was deposited on the stator transducer, control of the KOH concentration was not considered. This improvement of the PZT thin film will contribute to a higher motor performance. It is now our intent to fabricate a new transducer with a larger A factor.

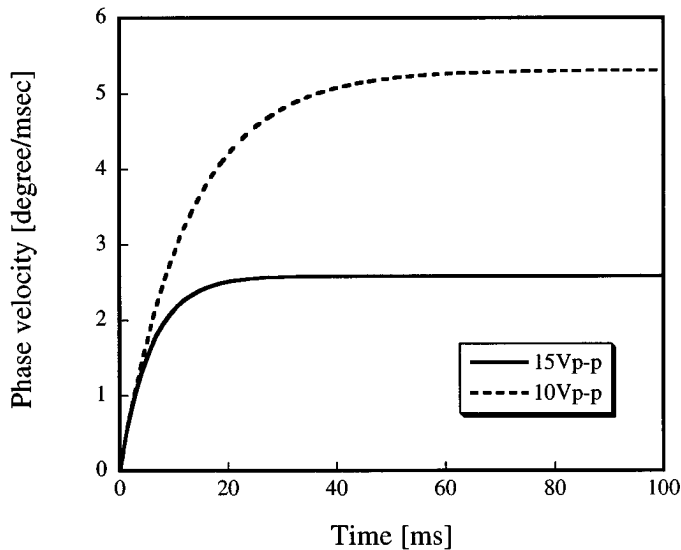


Fig. 22. The transient response of the motor.

TABLE V

THE CHARACTERISTICS OF THE MICRO ULTRASONIC MOTOR.

Driving voltage (Vp-p)	10	15
Time constant (ms)	5.7	13
Output torque (μNm)	7.0	6.3
Maximum speed (rpm)	430	880

IX. THE PERFORMANCE OF THE MOTOR

The performance of the motor was measured by using the Type 3 transducer fabricated by the single process hydrothermal method. The output torque was calculated from the transient response of the rotor. The angle of the rotor is measured by a high-speed camera, and the angle velocity is calculated from the position data. The preload generated by the spring was 4.4 mN. The total inertia of the rotors was 8.8×10^{-11} kg m². The results are shown in Fig. 22. The driving voltages were 10 Vp-p and 15 Vp-p to each electrode, with a 90 degree phase shift. By changing the phase shift to -90 degrees, the rotation direction was reversed as expected.

The characteristics of the motor are summarized in Table V. In spite of the different driving voltages, the output torque was almost the same. The maximum output torque of an ultrasonic motor is limited by the frictional force or output force generated by the transducer. The frictional force is calculated from the preload and frictional coefficient. The output force of the transducer is dependent on the piezoelectric factor of the PZT thin film. The results show that the output torque was determined by the frictional force.

As described above, the maximum output torque of the stator transducer was 26.0 μNm . The optimum preload will produce a larger output torque. The vibration energy will be efficiently transduced to driving force of the rotor revolution.

X. CONCLUSION

A single process hydrothermal method was proposed that does not require pretreatment nucleation process. The higher piezoelectric efficiency of the method contributed to an amplitude that was 2.5 times larger than that of the previous stator transducer fabricated by the nucleation and crystal growth processes.

From the result of bimorph fabricated by KOH control hydrothermal method, the piezoelectric factor d_{31} will be increased to -30 pC/N. This value is one-third of the bulk PZT. Based on the force factor calculation for stator transducer, however, it is clear that the piezoelectric factor is eight times smaller than that for the bulk PZT. This difference seems to indicate that the optimum reaction conditions for bimorph and stator transducers may be different. A PZT thin film with a piezoelectric factor d_{31} of -30 pC/N, should be able to be deposited on a stator transducer in the near future. Now we are trying to examine the relationship between precise KOH concentration and piezoelectric factor of the stator transducer.

ACKNOWLEDGMENTS

The authors would like to thank Mr. T. Kanda of The University of Tokyo for his assistance with the hydrothermal method for PZT thin film. This work has been supported by a JSPS Research Fellowship for Young Scientists.

REFERENCES

- [1] L. S. Fan, Y. C. Tai, and R. S. Muller, "IC-processed electrostatic micromotors," *Sens. Actuators*, vol. 20, pp. 41–48, 1989.
- [2] W. S. N. Trimmer and R. Jebens, "Harmonic electrostatic motors," *Sens. Actuators*, vol. 20, pp. 17–24, 1989.
- [3] K. Nakamura, H. Ogura, S. Maeda, U. Sangawa, S. Aoki, and T. Sato, "Evaporation of electric wobble motor fabricated by concentric build-up process," in *Proc. IEEE Inter. Workshop on Micro Electro Mechanical Systems*, pp. 374–379, 1995.
- [4] T. Akaki and M. Okabe, "(Nb-Tb)-F-B thin film magnet prepared by magnetron sputtering," in *Proc. IEEE Inter. Workshop on Micro Electro Mechanical Systems*, p. 244, 1996.
- [5] M. Kurosawa, K. Nakamura, T. Okamoto, and S. Ueha, "An ultrasonic motor using bending vibration of a short cylinder," *IEEE Trans. Ultrason., Ferroelect., Freq. Contr.*, vol. 36, no. 5, pp. 517–521, 1989.
- [6] K. Shimomura, T. Tsurumi, Y. Ohba, and M. Daimon, "Preparation of lead zirconate titanate thin film by hydrothermal method," *Jpn. J. Appl. Phys.*, vol. 30, no. 9B, pp. 2174–2177, 1991.
- [7] Y. Ohba, M. Miyauchi, T. Tsurumi, and M. Daimon, "Analysis of bending displacement of lead zirconate titanate thin film synthesized by hydrothermal method," *Jpn. J. Appl. Phys.*, vol. 32, part 1, no. 9B, pp. 4095–4098, 1993.
- [8] T. Morita, M. Kurosawa, and T. Higuchi, "An ultrasonic micro-motor using bending cylindrical transducer based on PZT thin film," *Sens. Actuators, A Phys.*, vol. A50, p. 75, 1995.
- [9] A. M. Flynn, L. S. Tavrow, S. F. Bart, R. A. Brooks, D. J. Ehrlich, K. R. Udayakumar, and L. E. Cross, "Piezoelectric micromotors for microrobots," *Proc. IEEE Ultrason. Symp.*, 1990, pp. 1163–1172.
- [10] G. A. Racine, R. Luthier, and N. F. de Rooj, "Hybrid ultrasonic micromachined motors," in *Proc. IEEE Inter. Workshop on Micro Electro Mechanical Systems*, pp. 128–132, 1993.

- [11] P. Muralt, M. Kohli, T. Maeder, A. Kholkin, K. Brooks, N. Setter, and R. Luthier, "Fabrication and characterization of PZT thin-film vibrator micromotors," *Sens. Actuators*, vol. A48, pp. 157–165, 1995.
- [12] Y. Xu and J. D. Mackenzie, "Ferroelectric thin films prepared by sol-gel processing," *Integr. Ferroelect.*, vol. 1, pp. 17–42, 1992.
- [13] T. Shiosaki, M. Fujimoto, M. Shimizu, M. Fukagawa, K. Nakaya, and E. Tanikawa, "Large-area growth of Pb(Zr,Ti)O₃ thin film by MOCVD," *Integr. Ferroelect.*, vol. 5, pp. 39–45, 1994.
- [14] T. Abe and M. L. Reed "RF-Magnetron sputtering of piezoelectric lead-zirconate actuator films using composite target," in *Proc. IEEE Inter. Workshop on Micro Electro Mechanical Systems*, pp. 164–169, 1994.
- [15] R. A. Roy, K. F. Elzold, and J. J. Cuomo, "Lead zirconate titanate films produced by 'facing targets' RF-sputtering," *Proc. Mater. Res. Soc. Symp.*, vol. 200, 1990, p. 82.
- [16] T. Morita, M. Kurosawa, and T. Higuchi, "Design of a cylindrical ultrasonic micromotor to obtain mechanical output," *Jpn. J. Appl. Phys.*, vol. 35, part 1, no. 5B, pp. 3251–3254, 1996.
- [17] M. Takahashi, M. Kurosawa, and T. Higuchi, "Direct frictional driven surface acoustic wave motor," in *Proc. Transducers '95 and Eurosensors IX*, Stockholm, Sweden, 1995, pp. 401–404.



Takeshi Morita was born in 1970. He received the B.Eng. and the M.Eng. degrees in precision machinery engineering from the University of Tokyo, Japan, in 1994 and 1996, respectively. He is currently a doctoral student of the Graduate School of Engineering.

His research interests are micro ultrasonic motor and PZT thin film.



Minoru Kuribayashi Kurosawa (M'95) (formerly Kuribayashi) was born in 1959. He received the B.Eng. degree in electrical and electronic engineering, and the M.Eng. and Dr.Eng. degrees from Tokyo Institute of Technology, Tokyo, in 1982, 1984, and 1990, respectively. He was a research associate at the Precision and Intelligence Laboratory, Tokyo Institute of Technology, Yokohama, Japan, beginning in 1984. Since 1992, he has been an associate professor at the Graduate School of Engineering, University of Tokyo.

His current research interests include ultrasonic motor, micro actuator, PZT thin film, SAW sensor and actuator, and 1-bit digital control system.



Toshiro Higuchi (M'87) was born in 1950. He received the B.S., M.S., and Dr.Eng. degrees in precision engineering from University of Tokyo, Japan, in 1972, 1974, and 1977, respectively. He was a lecturer at the Institute of Industrial Science, University of Tokyo, from 1977 to 1978, and an associate professor from 1978 to 1991. Since 1991, he has been a professor in the Department of Precision Engineering, University of Tokyo.

His research interests include mechatronics, magnetic bearing, electrostatic actuator, stepping motors robotics, and manufacturing.